Oxygen Adsorption on β-Cristobalite Polymorph: Ab Initio Modeling and Semiclassical Time-Dependent Dynamics†

M. Rutigliano,‡ C. Zazza,§ N. Sanna,§ A. Pieretti,§ G. Mancini,‡,§ V. Barone,|| and M. Cacciatore*,‡

CNR-IMIP, c/o Dipartimento di Chimica, Università di Bari, Via Orabona 4, 70126 Bari, Italy, CASPUR−Consorzio Interuniversitario Applicazioni Supercalcolo per Università e Ricerca, Via dei Tizii, 6b, 00185 Roma, Italy, and Scuola Normale Superiore di Pisa, Piazza dei Cavalieri, 7, 56126 Pisa, Italy

Received: July 13, 2009; Revised Manuscript Received: September 23, 2009

The adsorption dynamics of atomic oxygen on a model β-cristobalite silica surface has been studied by combining ab initio electronic structure calculations with a molecular dynamics semiclassical approach. We have evaluated the interaction potential of atomic and molecular oxygen interacting with an active Si site of a model β-cristobalite surface by performing DFT electronic structure calculations. As expected, O is strongly chemisorbed, $E_b = 5.57$ eV, whereas molecular oxygen can be weakly adsorbed with a high-energy barrier to the adsorption state of ~2 eV. The binding energies calculated for silica clusters of different sizes have revealed the local nature of the O,O_2−silica interaction. Semiclassical collision dynamic calculations show that O is mainly adsorbed in single-bounce collisions, with a smaller probability for adsorption via a multicollision mechanism. The probability for adsorption/desorption (reflected) collisions at the three impact energies is small but not negligible at the higher energy considered in the trajectory calculations, about $P_r = 0.2$ at $E_{kin} = 0.8$ eV. The calculations give evidence of a complex multiphonon excitation−deexcitation mechanism underlying the dynamics of stable adsorption and inelastic reflection collisions.

1. Introduction

The interaction of atomic and molecular oxygen with silica and silica-based materials under high temperature conditions can lead to various chemico-physical processes of great importance in many research areas of fundamental and technological interest. In particular, O_2 formation and desorption after oxygen atom recombination at silica surfaces is considered to be the main factor responsible for the thermal and structural damage to the thermal protection system (TPS) tiles on the space shuttles under re-entry conditions into the earth's atmosphere.[1] A large fraction of the exothermic energy delivered in the reaction can be transferred as heat flux to the surface, whereas the remaining energy is shared among the translational and the internal motions of the formed molecules. This energy sharing process is quite complex and not easy to quantify. Despite the intense research activity that has been developed to study the catalytic activity of various silica surfaces in dissociated oxygen gases,[2−4] the heat flux to the surface is still not accurately predictable.

O_2 formation has been investigated in several studies using various sources of atomic oxygen fluxes and various spectroscopic diagnostic tools to monitor oxygen atom density at the gas-surface boundary layer.[1] The main outcome of such investigations is the global recombination coefficient γ measured at different surface temperatures. In high-temperature regimes, close to the melting point of the silica samples used in the experiments, the reported data appear quite scattered because of the large uncertainty undergone in the experimental determinations.

However, it is worth noting that the atom recombination is not the only surface process responsible for the thermal heating of the solid substrate because many competing surface processes other than recombination can contribute to the global heat balance at the boundary layer. Atomic adsorption and adsorption/desorption processes can also be strongly exothermic because of the large chemisorption energy delivered in the interaction process. These processes are, quite generally, not included in kinetic modeling of dissociated air at the gas-surface boundary layer. Adsorption and adsorption/desorption processes have been much less investigated because of the obvious difficulties inherent in following these surface processes using in situ ultrafast spectroscopic techniques.

Apart from the TPS problem in aerospace, inelastic scattering of atomic O and N is a key step in many chemico-physical processes of great interest in several other research areas of basic and technological importance, from classical heterogeneous catalysis to thin film growth. Therefore, for example, atomic nitrogen incorporation into ultrathin SiO_2 films in plasma-assisted processes is of great importance in the microsemiconductor industry.[5,6] Nevertheless, there are no detailed collisional data on O and N adsorption on silica and oxide surfaces, whereas considerable experimental and theoretical activity has been devoted to inelastic scattering of atoms (mainly noble gases) from metallic surfaces.[7,8]

On the theoretical side, different kinetics schemes[9−11] have been applied to describe the kinetics of the chemistry at the gas−silica interface and then to simulate and predict the thermal response of silica or other TPS materials. In these studies, the various heterogeneous processes are described in terms of rate constants or cross sections so that some basic physical quantities, for example, the adsorption energies of the atomic and molecular

† Part of the "Vincenzo Aquilanti Festschrift".

* Corresponding author. E-mail: mario.cacciatore@ba.imip.cnr.it.
‡ CNR-IMIP.
§ CASPUR.
|| Scuola Normale Superiore di Pisa.

10.1021/jp9066026
Published on Web 10/21/2009

oxygen, activation energy barriers, and others, are treated as unknown parameters varied to fit the experimental data. As a consequence, the predictive power of such studies suffers from serious limitations. Moreover, despite the great deal of experimental and theoretical work, uncertainties still exist on collisional data relevant to the catalytic behavior of silica. More specifically, data relevant to the energy accommodation coefficient are largely incomplete, if not absent. These data can be difficult to obtain via experimental observations. On the contrary, molecular dynamics approaches in which all of the basic atomistic and electronic features of the interacting system are taken into account in a suitable manner when deriving the model, should be very helpful for understanding the catalytic mechanisms occurring at the interface in a well-defined way.

It is therefore the main aim of this work to describe at a very fundamental level the various collisional pathways underlying the dynamics of the O,O_2 interaction with silica. To this end, we have applied the semiclassical time-dependent molecular dynamics approach, which has been successfully applied in describing the catalytic routes of several elementary molecule−surface catalytic systems. This approach consists of two fundamental steps: (i) determination of a realistic interaction potential between the gas-phase atomic and molecular oxygen and the silica lattice atoms and (ii) use of a collisional model able to describe the dynamics of the gas-phase particles over the analytic PES derived from ab initio potential energy scans (PESs).

The first aspect is generally treated either by using simplified semiempirical models or by performing large-scale ab initio calculations using standard electronic structure methods developed in quantum chemistry. In a previous study,[12] a semiempirical potential for the O,O_2−silica interaction was derived on the grounds of physically motivated assumptions. Although rather crude, the calculated potential when inserted in the collisional semiclassical code was able, quite surprisingly, to account for the experimental global recombination coefficient γ determined in cell experiments.

In the present work, we follow the ab initio approach in the framework of the DFT−GGA (density functional theory−generalized gradient approximation) theory that we used when studying the N−silica interaction system.[13] According to the DFT approximation, the electron−electron interaction is treated in the mean-field way, whereas different approximations can be used to treat the electron exchange and correlation effects.

Because the evaluation of the full interaction potential for heterogeneous molecular systems is quite complex because of the large number of electrons and the multidimensional character of the potential energy surface, in this first contribution, we construct an ab initio DFT PES of reduced dimensionality by considering two parameters, that is, the normal distance of O,O_2 from the silica surface and the polar angle of approach. This potential contains the main features of the oxygen−silica interaction by including perpendicular O_{gas}−O−Si and angle-oriented O_{gas}−O interaction terms.

As far as the second aspect is concerned, the collisional method assumed in the dynamical simulation should be able to describe, as much as possible, the most fundamental behaviors of the reactive (atom recombination) and inelastic interactions of the oxygen−silica system. In particular, the energy shearing mechanism between the surface phonons and the gas-phase atoms should be included in the dynamics. Although it is of central importance in chemisorption, this latter aspect of the atom-surface reactivity is still a challenging issue. It is a matter of fact that in most calculations the interaction dynamics is performed on rigid surfaces, thus discarding the inelastic effects due to phonons and electron−holes excitations. The semiclassical method developed by us is able to handle, within a realistic approximation scheme, the most relevant features of the molecule−surface interaction, including the inelastic molecule−surface energy exchange processes.[14,15]

Furthermore, the characterization of the interaction potential of O_2 with β-cristobalite surface is also reported at quantum mechanics level showing a rather complex but at the same time very intriguing theoretical picture that clearly suggests, at least at the level of theory applied, the potential involvement of several electronic eigenstates along the sticking interacting trajectory.

In this first work, we focus on the adsorption, adsorption/desorption dynamics, and energetics of atomic oxygen interacting with a β-cristobalite surface, whereas a complete semiclassical study on the O_2 formation is in progress and will be presented in a future work.

2. Computational Setup

2.1. Density Functional Theory Calculations within Gradient-Corrected Approximation. Understanding chemical processes occurring at the interface represents a very intriguing and, at the same time, complicated task. To this end, theoretical and computational investigations of the sticking of atoms or molecules over a metallic (or crystal) surface is one of the most commonly accepted approach to examining local interactions and their relevance at the interface. Currently applied methodologies are often based on correlated electronic structure calculations employing either conventional wave-function-based approaches[16] or DFT methods.[17,18] In this respect, more approximate semiempirical techniques, for example, AM1[19] and PM3,[20] can model large systems (hundreds of atoms), but they are often inaccurate for a realistic description of chemical events in the presence of complex environment. DFT approaches in conjunction with GGA functionals provide a suitable and computationally appealing tool for obtaining accurate geometrical, thermodynamic, and kinetic parameters for a huge number of chemical processes under different conditions.[21] So having this in mind, we have recently and successfully applied DFT-based calculations for studying the N and N_2 interaction over β-cristobalite along ground-state potential energy profiles.[13] The basic picture emerged from our theoretical and computational investigation indicates that the local interaction is strongly affected and somewhat complicated, by the presence of different electronic spin eigenstates involved during the chemical attachment (to the surface) of the adsorbant.

Therefore, inspired by the above results, herein we have studied, using both DFT and Gaussian-type orbitals (GTOs), the O and O_2 interaction with a Si atom localized over β-cristobalite. To this end, we used the hybrid PBE0(GGA) functional[22] which is based on Perdew−Burke−Erzenrhof exchange-correlation functionals[23] in which a portion of Hartree−Fock exchange is added self-consistently to the DFT (PBE) contribution. Furthermore, it is worth noting that the selected functional does not contain any parameter fitted to reproduce atomic experimental data and, for this reason, is considered in literature as purely ab initio.

As already reported in our previous work,[13] several model systems of the silica surfaces have been properly taken into account keeping fixed the geometry of the silica surface at the experimental values and extending the (O/O_2)−$Si_xO_yH_z$ models up to $x = 17$, $y = 34$, and $z = 18$ (β-cristobalite, Figures 1 and 2). To study the O and O_2 interaction with a Si atom over the β-cristobalite, a potential energy surface scan has been made

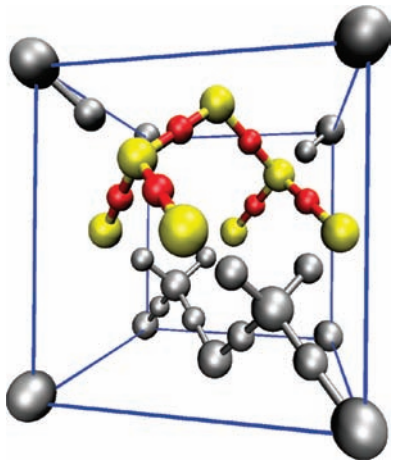

Figure 1. Skeleton of the Si_7O_{14} cluster reported in Figure 2, emphasized by colors, cleaved from the unit cell of β-cristobalite; silicon atoms are in yellow, oxygen atoms are in red.

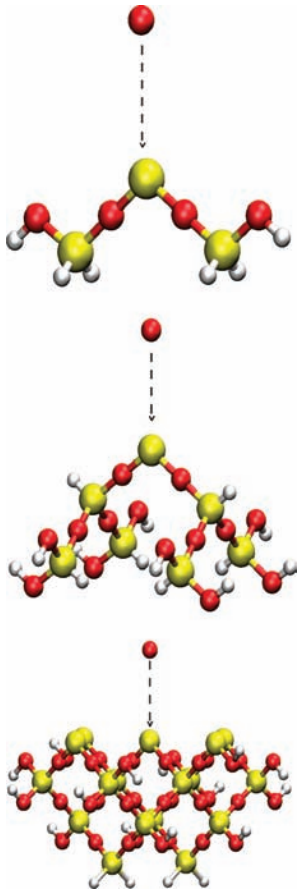

Figure 2. Cluster models of the O and O_2 (not shown) sticking interaction over the β-cristobalite polymorphs surface: upper panel, O···$Si_3O_4H_6$; middle panel, O···$Si_7O_{14}H_{14}$; bottom panel, O···$Si_{17}O_{34}H_{18}$. Silicon atoms are in yellow, oxygen atoms are in red, and hydrogen atoms are in white.

for each model depicted in Figure 2 (along the C_{2v} molecular symmetry axis) in the range $R_{O,Si}$ 1.00−4.00 Å; the O−O distance used in all O_2-surface PES calculations was kept fixed to 1.20 Å, close to the experimental value reported in literature,[24] along a perpendicular to the surface (sticking) direction of impact. Our theoretical modeling has been further extended to characterize oxygen(gas-phase)−oxygen(β-cristobalite) potential energy interaction at the interface. (See the molecular structures depicted in Figure 3.) PES calculations have been carried out

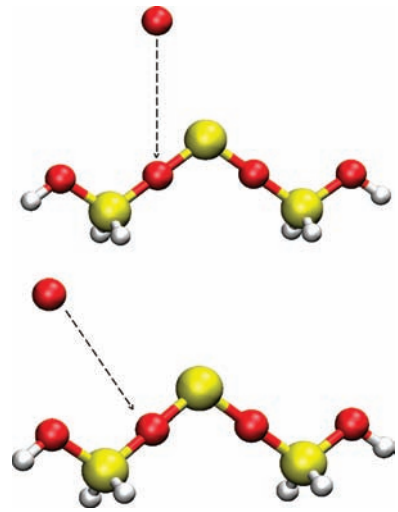

Figure 3. Starting geometries chosen to model two O(gas-phase)···O−$Si_3O_4H_6$ interacting systems over β-cristobalite; upper panel: conf1, lower panel: conf2. The arrow indicates the corresponding reaction coordinate (i.e., sticking) along the R_{O-O} interatomic distance. Colors as reported in Figure 1.

using a triple split valence Pople-style atomic basis set with additional diffuse sp functions and polarization d functions on heavy atoms, for example, 6-311+G*.[25] Furthermore, it is worth noting that for high-precision PESs, extremely tight convergence criteria were used, and an ultrafine grid has been chosen for DFT numerical integrations. PBE0/6-311+G* PES calculations are run on computational facilities at CASPUR (Rome) using the local installation of the Gaussian03 package.[26]

2.2. Semiclassical Time-Dependent Collision Dynamics. The method assumed to describe the interaction dynamics of atomic oxygen colliding with a silica surface is the semiclassical method. The method, described in detail in a number of publications and in the Billing's book,[15] has been applied to the study of several heterogeneous systems, including the H_2 dissociative chemisorption and H_2 formation after atom recombination on graphite (0001) and Cu(001) surfaces,[27,14] C oxidation catalyzed by Pt(111).[28] In ref 29, the distributions in angle and energy of Xe scattered inelastically from GaSe(001)[29] measured in molecular beam experiments were successfully interpreted within the semiclassical MD method. We like to remark here that the method provides a detailed knowledge of the multiphonon (and, eventually, of the electron−holes) inelastic processes that assist the dynamics of the chemical and physical phenomena due to the chemi- and physisorption of atoms and molecules on different substrates. This is, indeed, the most important behavior of the semiclassical approach.

According to this method, the dynamics of the gas-phase oxygen atom impinging the silica surface is described classically, whereas the lattice phonons are quantized. The dynamical coupling between the surface atom vibrations and the translational motion of the O atom is obtained by solving the classical Hamilton's equations of motion of the translational motion of the gas-phase oxygen in an effective Hamiltonian H_{eff} defined as

$$H_{\text{eff}} = \frac{1}{2m}(P_X^2 + P_Y^2 + P_Z^2) + V_0 + V_{\text{add}} + \Delta E_{\text{ph}} \quad (1)$$

where the first term is the kinetic energy of the atom with mass m, P_X is the X component of momentum, V_0 is the static

interaction potential between the gas-phase O and the silica atoms in their equilibrium positions, ΔE_{ph} is the energy exchanged between the interacting O and the substrate, and V_{add} is the dynamical contribution to the Hamiltonian because of the excitation/de-excitation processes of the perturbed phonon states. V_{add} is defined as the expectation value of the interaction potential V_{int} of the O−silica system over the total wave function of the phonon state: $V_{add}(t,T_S) = \langle \Psi_{ph}(t,T_S)|V_{int}|\Psi_{ph}(t,T_S)\rangle$, where t is the collisional time and T_S is the surface temperature. The time evolution of $|\Psi_{ph}(t,T_S)\rangle$ is obtained by solving the time-dependent Schrödinger equations of motion for a set of (3N-6) independent harmonic oscillators, N being the total number of atoms in the lattice, perturbed by the external forces exerted between the gas-phase atom and the silica surface. By further expanding the interaction potential, V_{int}, up to the first term of the phonon normal mode coordinates, the linearly forced harmonic oscillator (LFHO) analytical solution of the quantum equations of motion for the lattice phonons can be assumed, and the following expression for V_{add} is obtained

$$V_{add}(\bar{R},t,T_S) = \sum_k V_k^{(1)} \eta_k(t) \tag{2}$$

where $\bar{R}$ is the distance vector of the gas-phase atom from the surface, and $V_k^{(1)}$ is the first derivative of V_{int} with respect to the kth normal mode coordinate evaluated at the equilibrium position.[15,28] The time-dependent $\eta_k(t)$ coefficients are the phonon excitation strengths given in terms of the Fourier components of the external forces

$$\eta_k(t) = -\int dt'(\hbar\omega_k)^{-1} \frac{d}{d\rho_k}(\Delta E_k^+ + \Delta E_k^-) \times [I_{c,k}(t')\cos(\Theta_k(t')) + I_{s,k}(t')\sin(\Theta_k(t'))] \tag{3}$$

$$I_{c,k} = \int_{-\infty}^{+\infty} dt\, V_k^{(1)}(R(t))\cos(\omega_k t) \tag{4}$$

where $\Theta_k(t) \approx \omega_k t$. $\rho_k = (I_{c,k}^2 + I_{s,k}^2)/2\hbar\omega_k$, where ω_k is the frequency of the kth phonon mode. $\Delta E_k^{\pm} = \Delta E_k^{\pm}(\omega_k,T_s)$ is the energy loss ($\Delta E_k^+ > 0$)/gained ($\Delta E_k^- < 0$) by the oxygen atom due to the phonon excitation (+)/de-excitation(−) processes in the kth vibrational normal mode of the silica surface. The total energy exchanged between the translational motion of the oxygen atom and the phonons can be readily calculated as the sum of the individual contributions $\Delta E_k^{\pm}$ over the total number of phonon modes.

$$\Delta E_{ph} = \sum_k \sum_{n_k} \sum_{n_k^0} p_{n_k^0}(E_{n_k} - E_{n_k^0}) P_{n_k^0 \to n_k} = \sum_k (\Delta E_k^+ + \Delta E_k^-) \tag{5}$$

$(E_{n_k} - E_{n_k^0})$ is the energy exchanged in the transition $n_k \leftarrow n_k^0$ between the quantum states n_k^0 and n_k of the kth phonon mode. $P_{n_k^0}$ is the Boltzmann distribution of the phonon energies. $P_{n_k^0 \to n_k}$ is the transition probability. (See refs 15 and 28 for details.) $\Delta E_{ph} > 0$ indicates a net energy transferred to the silica surface.

The method, although quite involved from a formal point of view, is computationally feasible and provides a very realistic description of the molecule−surface interaction dynamics. The accuracy of the method mostly depends on the accuracy with which the interaction potential assumed in the scattering equations is known and the collisional energy regime explored in the dynamics.

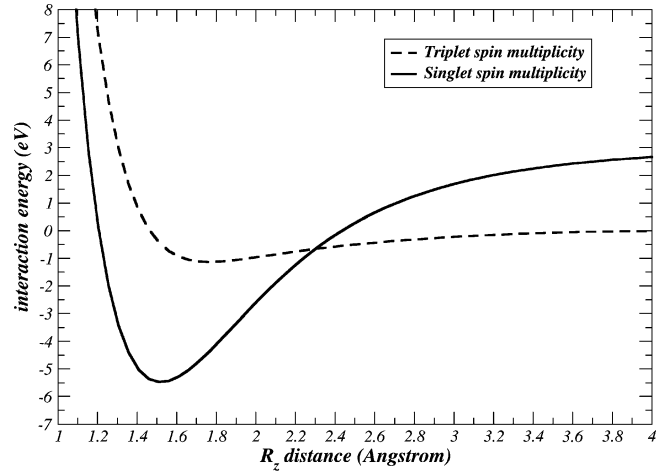

Figure 4. Oxygen atom interaction potential energy scan (PES) over the $Si_3O_4H_6$ cluster model of β-cristobalite surface; triplet (dotted line) and singlet (solid line) eigenstates of total electronic spin curves at PBE0/6-311+G* level of computation.

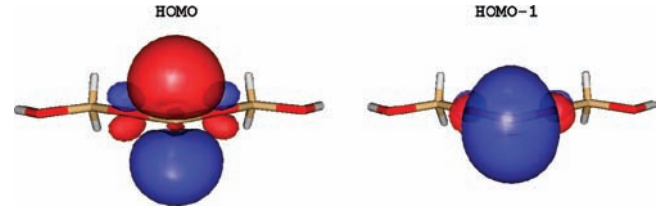

Figure 5. Highest occupied molecular orbital (HOMO) and HOMO-1 orbital (right panel) as obtained by PBE0/6-311+G* electronic wave function of the $^3[Si_3O_4H_6]$ cluster model. Isodensity surface equal to 0.05 electrons/bohr^3.

3. Results and Discussion

3.1. Interaction Potentials of O and O_2 over β-Cristobalite Surface. We first considered the interaction between an oxygen atom in gas phase and the Si atom of the $Si_3O_4H_6$ cluster model of the β-cristobalite surface. (See the upper panel reported in Figure 2.) It is quite evident that the direct pathway for the chemisorption of O over Si atom involves either singlet and triplet spin multiplicity as well as a smooth crossing around R(O−Si) = 2.3 Å between them. (See Figure 4.) The triplet PES is, however, more weakly bound than the singlet one; such a trend is most likely due to the formation of a strong polarized σ bond along the R_{O-Si} reaction coordinate and to the presence of a π SiO double bond on the singlet state.[31b] Indeed, our results clearly show that the spin singlet PES arises from the merging of two triplet moieties as follows: ^{3}P over O gas atom + $^3[Si_3O_4H_6]$ localized on the surface model. (See, for example, the highest occupied molecular orbital, HOMO and HOMO-1 in Figure 5.) The present PBE0/6-311+G* PES calculations predict a binding energy of −5.47|−5.60|−5.57 eV (as a function of the cluster size) with a minimum lying at R_{O-Si} = 1.52 Å. Moreover, the asymptotic energy difference between the two potential energy curves (in Figure 4) has been found to be equal to 2.67 eV, which is exactly the potential energy difference between $^3[Si_3O_4H_6]$ and $^1[Si_3O_4H_6]$ free clusters (where in both profiles, the O appears in its own ^{3}P ground state). It is also important to note that our results are in agreement with previous findings using the Perdew−Wang 91 (PW91) functional[30] with plane waves and periodic boundary

TABLE 1: *R*(O−Si) Minimum Distances and Interaction Energies (Termed as B_e and Reported in electronvolts) for the O−$Si_xO_yH_z$ Model Systems of the Oxygen Sticking over *β*-Cristobalite (See Figures 1 and 2) Computed with the PBE0/DFT Functional and 6-311+G* Atomic Basis Set

system *β*-cristobalite	B_e/eV	R_{min} (O−Si)/Å
O−$Si_3O_4H_6$	−5.47	1.52
O−$Si_7O_{14}H_{14}$	−5.60	1.51
O−$Si_{17}O_{34}H_{18}$	−5.57	1.52

conditions while keeping frozen the *β*-cristobalite polymorph. In fact, in ref 31, the binding energy computed considering the atomic oxygen sticking on top of Si (Figure 2) was found to be −5.6 eV at R_{O-Si} = 1.56 Å. (See the curve termed as T1 in Figure 2a of Arasa et al. in ref 31a.) As a final step, we also checked that the counterpoise corrections for basis set superposition error (BSSE) remain confined within the chemical accuracy (i.e., <1 kcal/mol in the whole range of the calculated PES).

To perform a quantitative examination of our quantum mechanical results, we report in Table 1 the most relevant energetic and structural parameters increasing the size of the O−$Si_xO_yH_z$ interacting model surface. (See the molecular clusters depicted in Figure 2.) As already observed in the presence of a N atom over the same $Si_xO_yH_z$ models,[13] at increasing dimension of the model cluster, the R_{min}(O−Si) distance remains almost constant, whereas the binding energy increases up to −5.57 eV (O−$Si_{17}O_{34}H_{18}$). In light of this finding, it is, however, possible to consider the $Si_7O_{14}H_{14}$ cluster model having a binding energy of −5.60 eV (Table 1) as rather accurate in the description of the interaction potential between the oxygen atom and the silicon atom at the gas/surface interface. (See Table 1.) Although the smallest cluster (i.e., $Si_3O_4H_6$) correctly describes all induced electronic rearrangements involved in the collisional event, it tends to underestimate the binding energy moderately by 0.13 eV (−5.47 eV). On the basis of such a result, population analysis confirms that in the current case the chemical interaction on the surface is mainly confined over the on-top Si and the nearest oxygen atoms.

As far as the O_2−$Si_xO_yH_z$ surface model is concerned, we adopted the same size-scalable approach as that reported in detail for the oxygen case. In Figure 6, we report the O_2−$Si_3O_4H_6$ PES scans obtained at the PBE0/6-311+G* level of computation. At first, our calculated PES scans show a rather complicated interaction route between the incoming O_2 molecule and the model surface involving (as already observed in the previous cases) both singlet and triplet magnetic spin eigenstates. The oxygen molecule, initially in its own electronic ground state ($X^3\Sigma_g^-$) at large distance from the surface, provides a strong repulsive potential energy profile while approaching the ^{1}[$Si_3O_4H_6$] cluster model. (See curve A in Figure 6). Afterward, a deeper inspection of our data indicates, as already observed for ($^3N_2$/$^1N_2$) and *β*-cristobalite,[13] that under our simulation conditions the interaction is strongly "spin-state-selected", showing a remarkable discrimination in the electronic configuration of the whole investigated system. The analysis of the electronic spin population carried out on the converged electronic wave functions along the computed PES scans evidence: (i) A first crossing point located at almost R_{O-O-Si} = 2.1 Å (Figure 6), where the O_2 undergoes an electronic change from $X^3\Sigma_g^-$ to the first singlet electronic excited state with unpaired valence electrons, $^1\Sigma_g^+$, accompanied by a local magnetic change also occurring onto the surface model (e.g., (^{1}[$Si_xO_yH_z$]/^{3}[$Si_xO_yH_z$]). The resulting triplet PES (curve C), composed of the O_2($^1\Sigma_g^+$) and ^{3}[$Si_xO_yH_z$] moieties, is binding toward O_2 absorption because the two unpaired electrons of Si atom at the surface can be involved in donor bonding with the incoming gas molecule. (ii) At shorter (O−O)−Si interatomic distances, the lowest potential energy profile has a singlet spin multiplicity, which combines O_2($^3\Sigma_u^+$) and ^{3}[$Si_xO_yH_z$] fragments (curve D).

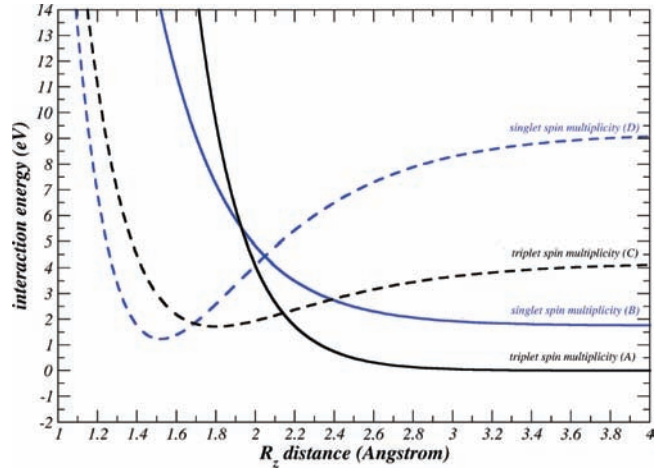

Figure 6. O_2 potential energy scan (PES) over the $Si_3O_4H_6$ cluster model of *β*-cristobalite surface; R_z parameter indicates the distance between the nearest to the surface oxygen atom of the O_2 and the closest interacting Si. Triplet (blue lines) and singlet (black lines) eigenstates of total electronic spin curves at PBE0/6-311+G* level of computation.

With respect to the previous triplet PES, at the crossing point, whereas the *β*-cristobalite model retains its electronic configuration ^{3}[$Si_xO_yH_z$], the change in spin state (triplet/singlet) is due to a local electronic rearrangement within the O_2 molecule. In this respect, it is interesting to note that the O_2 ($^3\Sigma_u^+$) species is the most strongly bound in terms of potential energy and also shows the shortest (O−O)−Si interatomic distance. (See Figure 6.) At last, we also report the potential energy curve regarding the oxygen molecule in the $^1\Delta_g$ state (curve B in Figure 6). As can be clearly seen, closed shell electronic moieties, that is, O_2($^1\Delta_g$) and ^{1}[$Si_xO_yH_z$], show a purely repulsive behavior basically arising from electron−electron Coulomb repulsive interaction. The final assembly of the resulting PESs regarding the O/O_2−$Si_3O_4H_6$ (*β*-cristobalite) systems, calculated at the PBE0/6-311+G* level of computation, are reported in Figure 7, where a comparison with the larger cluster $Si_7O_{14}H_{14}$ clearly shows the numerical accuracy of the computed PESs. Note that the same intriguing physical picture has been observed when PES scans are calculated using the B3LYP functional and 6-311+G* basis set.

However, it is important to note that although our results provide a first-principles-based interaction pattern for O_2 molecule over such a polymorph, to give an exhaustive response to this interesting issue, more comprehensive calculations are necessary to sample all of the possible interacting trajectories basically differing for the mutual orientation of the O_2 molecule. In this context, the flexibility of the O−O distance is also expected to play a key role in modulating the potential energy surfaces in the interaction regime.

Using the present potential to simulate the O_2 formation would be very reductive and not fully appropriate. Therefore, the O + O reaction dynamics on silica will be the object of a subsequent publication. Rather, in this work, we focus on the atomic oxygen adsorption dynamics, which is by no means affected by the O_2−silica reactive branch of the complete PES.

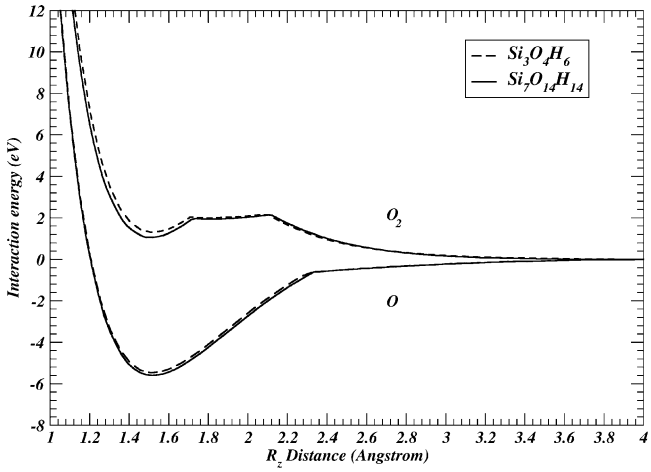

Figure 7. Calculated, at the PBE0/6-311+G* level of computation, O/O_2 potential energy scan (PES) over the $Si_3O_4H_6$ cluster model of the β-cristobalite surface (dotted lines); note that the comparison with the $Si_7O_{14}H_{14}$ cluster is also reported (solid lines).

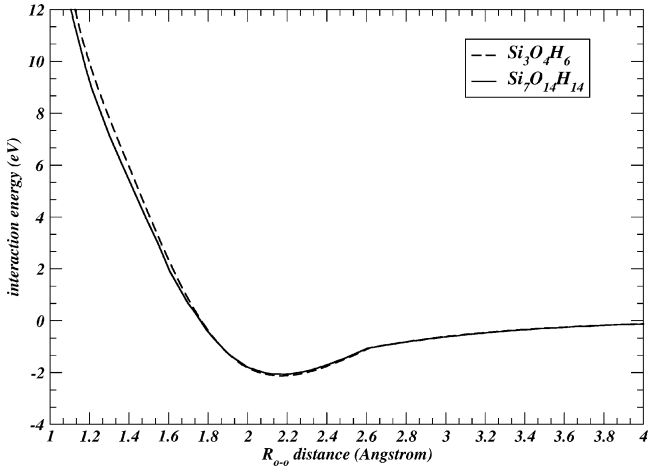

Figure 8. PBE0/6-311+G* calculated O(gas-phase, conf1)−O(β-cristobalite) potential energy scan (PES) over the $Si_3O_4H_6$ cluster model of β-cristobalite polymorph surface (dashed line, see the molecular structure depicted in Figure 3, upper panel); note that a comparison with $Si_7O_{14}H_{14}$ cluster is also shown (solid line).

However, it must be also remarked that the theoretical modeling along the R_{O-O} collisional coordinate (see the initial conformation, as reported in Figure 3) provides potential interaction energy curves that clearly indicate that along the sticking direction of impact a chemisorption process can occur without any potential energy barrier (Figure 8), but the resulting bond is weak if compared with a prevalent O−Si (on top over the surface) interaction. In this respect, the O(gas-phase)−O(β-cristobalite) electronic repulsion forces are balanced by Si−O local interaction at R_{O-O} intermediate distances. As already emerged (see, for example, the curves depicted in Figure 4) at long distances the O−(O−β-cristobalite) system is composed of O as ^{3}P and ^{1}[$Si_xO_yH_z$], whereas at R_{O-O} distance <2.7 Å (R_{O-Si} = 2.2 Å), the surface model system changes its electron spin magnetic state from closed-shell singlet to open-shell triplet. (See Figure 8.) Therefore, a binding energy of −2.13 eV at R_{O-O} = 2.17 Å and R_{O-Si} = 1.75 Å is found considering the $Si_3O_4H_6$ cluster, and a binding energy of −2.08 eV at R_{O-O} = 2.18 Å and R_{O-Si} = 1.74 Å is found for the $Si_7O_{14}H_{14}$ cluster. At last, it should be noted that when the incoming atom interacts with the β-cristobalite surface along a trajectory having an angle of 90.0° between the O and the on-top Si atoms of the polymorph substrate (termed as conf2, see lower panel in Figure 3), a repulsive behavior composed of singlet (at shorter distances) and triplet eigenstates is observed in our DFT-based calculations for the presence of a large excess of electronic density along such an impact direction. (See Figure 9.)

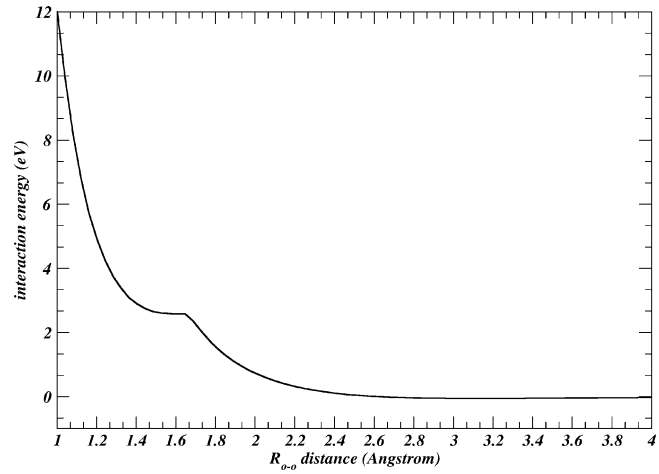

Figure 9. PBE0/6-311+G* calculated O(gas-phase, conf2)−O(β-cristobalite) potential energy scan (PES) over the $Si_3O_4H_6$ cluster model of β-cristobalite polymorph surface (see the molecular structure depicted in Figure 3, lower panel).

In summary, for the chemisorption of oxygen atom over β-cristobalite surface along the sticking direction, we have found that a change in the spin-state (i.e., triplet-singlet) should occur, according to previous published data.[31] We also find, for the first time, that the impact of an oxygen molecule over the silicon atom at the interface most likely involves three different electronic eigenstates as well as potential surfaces crossing between them. This means that looking at present results and by analogy to the interaction patterns found for N and N_2 over the same substrate,[13] the catalytic activity over the β-cristobalite surface is strongly modulated by the flexibility of the electronic degrees of freedom during the mutual interaction with incoming "objects". However, it can be noted that for a theoretical modeling going beyond our current representation, relativistic effects (i.e., spin orbit coupling) should be included, in particular, within curve crossing regions sampled by our DFT-based calculations.

Attempting to get some basic insight into the dynamics of O_2 formation on a silica surface, in ref 12b, the interaction potential for O_2−β-cristobalite system was derived semiempirically. The same procedure was followed for O_2−β-quartz.[12a] Quite surprisingly, the calculated semiclassical recombination coefficients were in good agreement with the experimental values. However, as stressed in ref 12a,b, this agreement must be taken with precaution because collisional data calculated in MD simulations cannot be, in principle, directly compared with results determined in cell experiments.

It must be also remarked that the semempirical potential was determined to simulate the O_2 formation over a silica surface, and it cannot be considered appropriate to describe the adsorption dynamics of O on a clean silica surface. The semiempirical potential cannot account for the complex electron spin dependence found in the DFT calculations. Rather, it fits quite well the DFT potential branch of the triplet fundamental state of O_2. The O atoms recombination dynamics over the DFT PES is expected to be quite different.

In the next section, we extend our study by introducing the minimum energy interaction patterns found for the oxygen atom

along the sticking impact coordinate (Figures 7 and 8) over β-cristobalite surface in the atomistic force field needed for semiclassical molecular dynamics simulations.

3.2. Oxygen Atom Adsorption Dynamics over β-Cristobalite Surface. In addition to the PES calculation discussed in the previous section, the complete dynamic simulation of molecular surface processes, described within the semiclassical method briefly outlined above, requires the solution of two main steps: (i) First, the phonon dynamics of the silica surface is studied, and the corresponding phonon eigenvectors and eigenvalues are calculated. (ii) Second, the full dynamics of the O−silica interaction is carried out by self-consistently solving the Hamilton's equations of the O atom and the dynamics of the phonons (that is, by computing the phonon excitation strengths of eqs 3 and 4 at each time step of the semiclassical trajectory).

The β-cristobalite surface model assumed in the scattering calculations was built up starting from the known arrangement of the silicon and oxygen atoms in the lattice bulk of the unit cell[32] such that the stoichiometry and neutrality of the crystal are fulfilled. Therefore, structural defects due to surface reconstruction were not considered. The existence of a complex reconstructed surface layer has been demonstrated in molecular dynamics studies of vitreous silica.[33] The 3D surface slab consists of 149 atoms in 10 layers that correspond to a 2×2 unit cell (cell parameter $a = 7.1161$ Å taken from Wyckoff[32]). The area of the uppermost layer is 202.55 Å^2.

The interaction potential between the Si and O atoms in the crystal lattice was given as the sum of two components: the purely repulsive short-range Born−Mayer−Huggins potential and the long-range screened Coulomb component exerted between the nearest and next-nearest neighbor lattice atoms. Using the potential parameters given in ref 33, the phonon frequencies and phonon eigenvectors in the scattering equations were calculated by numerically diagonalizing the 3D force constant dynamical matrix written for the β-cristobalite cluster geometry. The obtained phonon frequency distribution compares well with the typical band structure of the phonon density of states obtained for silica from molecular dynamics calculations.[34]

The interaction potential assumed in the semiclassical scattering equations is expressed as the sum of pairwise atom−atom interactions between the gas-phase oxygen atom and the Si and O of the silica surface

$$V_{\mathrm{O-SiO_2}} = [\sum_{i=1}^{N_{\mathrm{Si}}} V_{\mathrm{O-Si}}]f_t + [\sum_{i=1}^{N_{\mathrm{O}}} V_{\mathrm{O-O}}](1 - f_t) \quad (6)$$

$$f_t = 1 - 1.17 \tanh \sqrt{(X_0^2 + Y_0^2)} \quad (7)$$

where f_t is a switching function and (X_0,Y_0) are the coordinates of the gas-phase atom in the $(X-Y)$ plane of the assumed frame of reference. The DFT $V_{\mathrm{O-Si}}$ and $V_{\mathrm{O-O}}$ interactions presented in the previous section were fitted by Morse potentials

$$V_{\mathrm{O-Si}} = D_{\mathrm{O-Si}} e^{-p_{\mathrm{O-Si}}(R_{\mathrm{O-Si}}-r_1)}(e^{-p_{\mathrm{O-Si}}(R_{\mathrm{O-Si}}-r_1)} - 2) \quad (8)$$

$$V_{\mathrm{O-O}} = D_{\mathrm{O-O}} e^{-p_{\mathrm{O-O}}(R_{\mathrm{O-O}}-r_2)}(e^{-p_{\mathrm{O-O}}(R_{\mathrm{O-O}}-r_2)} - 2) \quad (9)$$

where $R_{\mathrm{O-O}}$ is the distance between the impinging O atom and the O lattice atoms. The Morse parameters, $D_{\mathrm{O-Si}}$, $p_{\mathrm{O-Si}}$, $D_{\mathrm{O-O}}$, $p_{\mathrm{O-O}}$, r_1, and r_2, are reported in Table 2.

In Figure 10, the analytical interaction potential for oxygen interacting with a Si lattice atom in the perpendicular geometry is reported as a function of the O−Si distance. The reference ab initio potential is also shown.

Simulation of the O−silica interaction system is quite simple. Propagation of the collisional trajectories requires the definition of the initial position coordinates and momenta of the O atom approaching the silica surface from the gas phase. We define the initial conditions with respect to a Cartesian frame of reference centered on a Si surface atom and having the Z axis normal to the silica surface pointing out toward the vacuum. The $(X-Y)$ plane lies on the surface top layer. In the simulation, the O atom is initially placed at a distance $Z = 8$ Å into the asymptotic free region. In this preliminary study, we focus on the dynamics of the O atom approaching the surface with a specific initial geometry on the topmost Si site of β-cristobalite. Because of the reduced dimensionality of the calculated O−silica interaction potential, we cannot extend the adsorption dynamics on the lattice sites of the unit cell other than the on-top Si site. Therefore, we assume that the gas-phase O approaches the silica surface perpendicularly to the surface plane (polar angles $(\vartheta,\varphi) = (0,0)$) with a given kinetic energy, E_{kin}. The initial position coordinates (X,Y) are chosen randomly within an aiming area of 2.0 Å^2 centered on the active silicon site.

The dynamics was carried out at three impact energies, E_{kin}= 0.2, 0.5, and 0.8 eV, and the temperature of the silica surface was kept constant at $T_S = 1000$ K. For each impact energy, a batch of 500 trajectories was performed, which ensures a numerical convergence of the calculated adsorption probabilities of ~5%. An integration time step of 5×10^{-16} s was used in the trajectory propagation. The trajectories are assumed to be stable if the total energy is conserved within 1%.

The interaction of O with silica being relatively simple can lead to three basic surface processes: (i) Direct desorption and indirect adsorption/desorption. We assume that O desorbs when it is scattered from the silica surface far into the free space, with the Z coordinate >8.0 Å in the final condition of the trajectory. (ii) Adsorption process, which can be of two types:

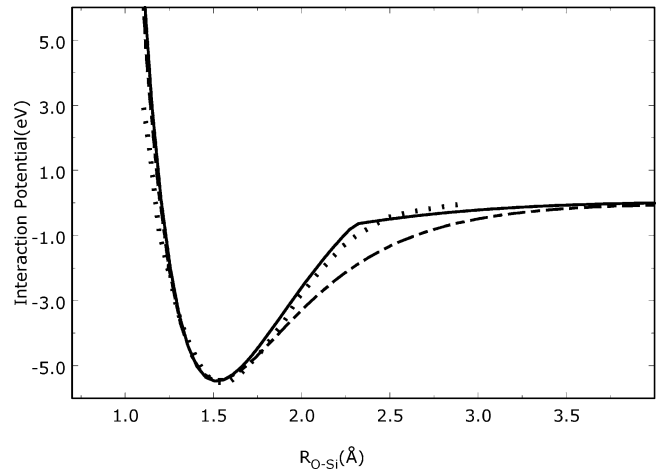

Figure 10. O−Si interaction potential as a function of the O−Si distance. The gas-phase O atom approaches the silica surface perpendicularly on top of the Si lattice atom. Full line: DFT calculations; dashed line: analytical fit; dotted line: results obtained in ref 31.

TABLE 2: Best-Fit Potential Parameters of Equations 8 and 9

$D_{\mathrm{O-Si}}$ (eV)	$p_{\mathrm{O-Si}}$ (Å^{-1})	r_1 (Å)	$D_{\mathrm{O-O}}$ (eV)	$p_{\mathrm{O-O}}$ (Å^{-1})	r_2 (Å)
5.34	2.1	1.53	0.9	1.64	3.24

TABLE 3: Average Semiclassical Probabilities for Inelastic Adsorption and Reflection Processes Due to O−Silica Interaction at Three Impact Energies (T_S = 1000 K)

E_{kin} (eV)	adsorption	reflection
0.2	0.941	0.058
0.5	0.822	0.178
0.8	0.787	0.212

direct adsorption, in which the oxygen atom is trapped at the surface after a single collision, and indirect adsorption due to multiple collisions with the silica substrate. In both cases, we assume that O is adsorbed when the energy available to the O atoms to escape from the chemisorption potential well, ΔE_{esc}, is less than the effective potential, V_{add}, experienced by the oxygen at a specific interaction time. ΔE_{esc} is defined as: $E_{tot} - \Delta E_{ph} - E_0$, where E_0 is the zero-point energy of the chemisorbed atom. $E_{tot} = E_{kin} + V_{add} + \Delta E_{ph} + V_{int}$ is the total energy, and E_{kin} is the kinetic energy of the gas-phase O atom. Furthermore, a second criterion can be followed by which O is adsorbed whenever the Z component of the atom reaches the chemisorption distance, Z_{ad} = 1.54 Å, and the component of the momentum along the Z direction is negative for a sufficiently long time, that is, just a few picoseconds. (iii) Absorption, when the oxygen colliding with the silica is finally trapped into a subsurface site.

Adsorption as well as absorption collisions are dominated by a strong coupling of the translational motion of the impinging O atom with the silica phonons. Because of this strong coupling, these collisions can be numerically unstable so that they cannot be followed for much time. (The criterion of total energy conservation is no longer fulfilled when O sits at the surface for any longer than several picoseconds.) This aspect is well-known and introduces some limitations to the feasibility of molecular dynamics approaches to surface processes occurring on a time scale longer than 10^{-12} sec, whereas Monte Carlo kinetics approaches or mixed MD and stochastic methods based on the generalized Langevin approach are more suitable for surface processes with long residence times. Molecular dynamics methods are well suited to studying surface desorption and surface reactions.

In Table 3, the probabilities for inelastic reflection and adsorption are reported at the three collisional energies explored in this study. The reported values are averaged over a batch of collisional trajectories.

We note that the desorption channel is scarcely effective, the great majority of the collisional events ending with O adsorbed. Our results agree well, also at a quantitative level, with the results recently reported by Sayòs et al.[31] on the same system but using a different collisional approach. That work also showed that the effects of both the incident angle and the surface temperature on the adsorption process are very weak.

According to our analysis, the O−silica interaction is dominated by direct adsorption where the oxygen atom undergoes a single collision before being adsorbed. However, a small but significant fraction of atoms rebounds several times on the silica surface before a stable adsorption. In Table 4, the average probabilities for single and multistep adsorption are reported at the three impact energies E_{kin}.

It is worth noting that the probability for multibounce adsorption increases significantly at the lowest impact energy. This is a consequence of the longer residence time spent on the surface in low-energy collisions.

Although the kinetics of these processes is relatively simple, the dynamics can be quite complex depending, in particular, on the relaxation time typical of a specific process.

TABLE 4: Probabilities for Single- and Multistep Adsorption in O−Silica Interaction (the Gas-Phase O-Atom Perpendicularly Impacts the Silica Surface) (T_S = 1000 K)

E_{kin} (eV)	adsorption (single step)	adsorption (multi step)
0.2	0.725	0.216
0.5	0.687	0.135
0.8	0.721	0.066

Figures 11a and 12a show a typical trajectory of an indirect adsorption and of a reflection process, respectively. Here the Z component of the gas-phase O-position vector is plotted as a function of the collisional time in units of τ, $1\tau = 10^{-14}$ s. In these Figures, the energy transferred to the phonons, ΔE_{ph}, is also reported at each trajectory time.

Adsorption and adsorption−desorption processes at the silica surface are assisted by the multiphonon excitation−deexcitation processes. In fact, analysis of the collisional trajectories shows that the energy exchange between the gas-phase oxygen and silica plays a key role in the dynamics of the interaction. This is shown in Figures 11b and 12b, where the energy exchanged with the phonons and the translational energy of the oxygen atom is reported as a function of the collisional time for the adsorption and reflection trajectories plotted in Figures 11a and 12a, respectively. In Figures 11b and 12b, the time evolution of ΔE_{ph} and E_{kin} is reported for a narrow time interval around the collisional turning points of the trajectories. At the collisional turning point, the oxygen atom reaches the closest distance from

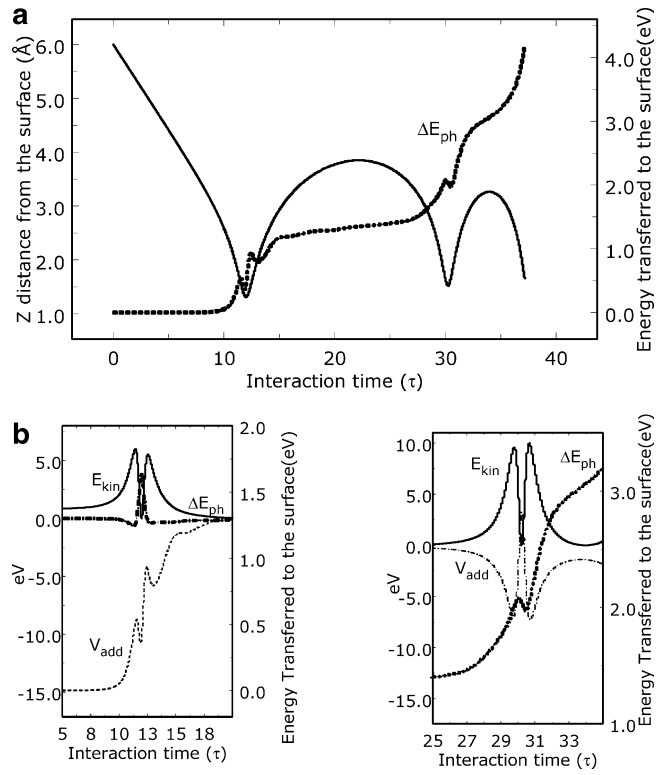

Figure 11. (a) Time evolution of a typical trajectory for a multistep adsorption process. The Z normal coordinate as a function of time for O atom impinging on the surface is reported as a function of the collision time (left-hand scale). The energy exchanged with the surface (dotted line) is also reported on the right-hand scale. E_{kin} = 0.8 eV and T_S = 1000 K. (b) The kinetic energy E_{kin} of the interacting O atom and the energy exchanged with the silica surface ΔE_{ph} (right-hand scale) are reported as a function of time for the narrow time-interval around the two collisional turning points of the two-step adsorption trajectory shown in Figure 11a. The effective potential V_{add} is also shown.

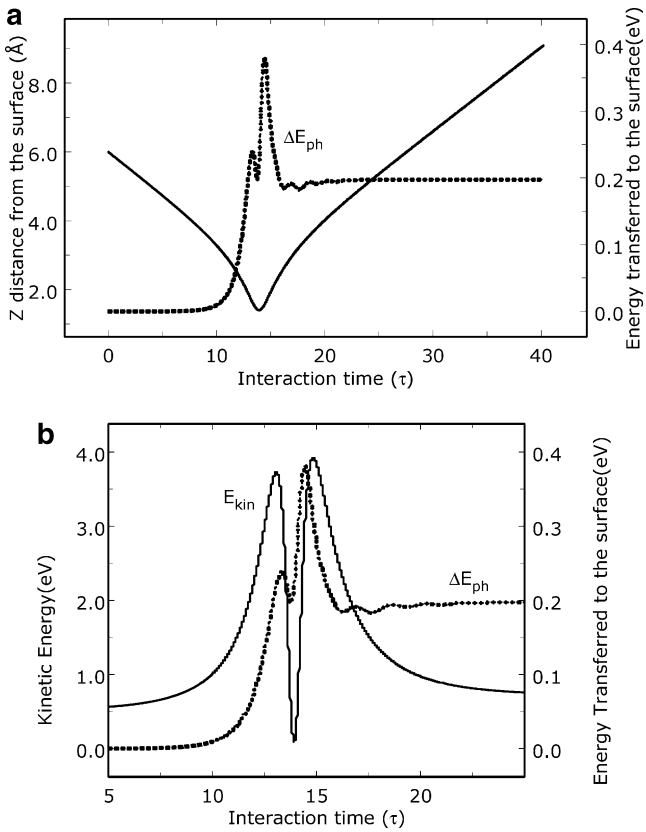

Figure 12. (a) Same as Figure 11a but for a reflection process. $E_{kin} = 0.5$ eV and $T_S = 1000$ K. (b) E_{kin} and ΔE_{ph} as a function of time for the narrow time interval around the collisional turning point of the reflection trajectory in Figure 12a.

TABLE 5: Average Energy Transferred to the Silica Phonons, ΔE_{ph}/eV, in Single-Step Adsorption and Reflection of Atomic Oxygen Interacting on Top of a Si Lattice Site ($T_S = 1000$ K)

E_{kin} (eV)	single step adsorption	reflection
0.2	0.237	0.373
0.5	0.375	0.358
0.8	0.548	0.478

the silica surface, and this corresponds to the maximum interaction condition and, as a consequence, to the maximum energy exchange.

We note that the oxygen atom is first accelerated into the chemisorption potential well ($V_{add} < 0$) gaining kinetic energy. However, as the atom comes closer to the surface, coupling to the phonons becomes more effective so that there is a net energy transfer from the O to the phonons. As the dynamics goes on and the oxygen comes to closer to surface, the oxygen is scattered out from the potential well ($V_{add} > 0$). The kinetic energy gained by the oxygen when scattered from the surface is, immediately afterward, transferred to the phonon, and the particle again loses kinetic energy. If the energy loss is large, then the oxygen atom can be trapped once again by the surface before being stable adsorbed (as in the two-step adsorption trajectory in Figure 11a), or it can definitely emerge into the gas phase. (See Figure 12a.) We note that when O is inelastically scattered in the gas phase, almost all of its initial kinetic energy is delivered to the surface.

Table 5 reports the average energy transferred to the silica surface for direct and reflection collisions at the three impact energies considered in the dynamic simulation.

As can be noted, the energy transferred to the silica surface is large. As a consequence a lattice atom rearrangement and geometry changing of the silica slab along the collisional trajectories is quite probable. Furthermore, an important result pointed out in the previously reported DFT electronic structure calculations is the localized character of the O−silica interaction potential, so that a similar behavior should be expected for the adsorption dynamics. Local effects in the adsorption dynamics can be pointed out within the semiclassical method. In fact, the expectation values of the lattice atom displacements induced by the O−silica interaction can be calculated at the end of each collisional event. This enables us to identify the silica atoms most involved in the dynamics (and the impact the surface reorganization could have on the energy-exchange mechanism that assists the interaction dynamics). This interesting aspect of oxygen−silica interaction dynamics will be explored in the course of our ongoing study on O_2 formation on silica.

4. Concluding Remarks

DFT electronic structure calculations performed in this work within the size-scalable cluster approach have highlighted the localized nature of the O,O_2−silica interaction, a behavior also confirmed by the very good agreement found between the present cluster and periodic slab calculations appearing in the literature. This effect is somehow expected because of the tetrahedral structure of the silica network and the strongly covalent, although partially ionic, character of the Si−O bonds. Calculations show that O is chemisorbed on a Si active site and that the binding energy of the gas-phase atomic oxygen interacting with the lattice O atoms depends sensitively on the interaction geometry.

The localized character of the interaction, along with the angular dependence of the O−O interaction, point toward a multidimensional character of the complete PES and, as a consequence, toward the necessity for further calculations involving a higher number of potential coordinates (specifically, the planar X,Y coordinates defining different sites of adsorption). Calculations of this nature are underway and will be presented in a future work.

A further aspect that needs to be discussed concerns the long-range interactions due to the charged silica atoms and quadrupole charge separation in O_2. Notably, these interactions are not described within the DFT approximation but could play a role in the adsorption processes.

Coupling the fundamental information obtained in the quantum chemistry calculations to the semiclassical collisional model provides information on some aspects of the O−silica interactions of fundamental and applicative relevance. This was achieved in the second part of this work, where the dynamics of atomic oxygen scattered inelastically from a silica surface was studied for a specific initial geometry of the gas-phase O atom. The results show that the dynamics is dominated by the inelastic adsorption processes, a result that is in line with the strong chemisorption potential well found for the O interaction geometry considered in the calculations. Therefore, a flux of atomic oxygen directed normally toward a silica surface will be almost completely adsorbed at the surface, whereas a small fraction would be reflected back into the gas-phase. Trajectory analysis reveals that adsorption proceeds mainly via a direct single-bounce mechanism, with ~12% of the adsorption process occurring after several surface bounces. These sticking adsorption collisions take place over a longer time scale (several picoseconds).

A further remarkable result concerns coupling to phonons; it turns out that the inelastic phonon process is important,

particularly at the lower impact energy and cannot be discarded in the dynamics. For all collisional events examined, we observe a net energy transfer from the gas-phase O atom to the silica surface.

Acknowledgment. This research is financially supported by the Italian Space Agency (ASI) in the framework of the CIRA-IMIP project "CAST- Innovative Aero-thermodynamic Configurations for Systems of Spatial Transport" and by CASPUR-Rome, which provided part of the computer facilities used in this work under the grant "Bandi 2007".

References and Notes

(1) *Experiments, Modeling, and Simulations of Gas-Surface Interactions for Reactive Flows in Hypersonic Flights*; Proceedings of the AVT-142 RTO AVT/VKI Lecture Series, von Karman Institute, Rhode St. Genèse, Belgium, Feb 6−10, 2006; Chazot, O., Rini, P., Eds.; RTO/NATO: Neuilly-Sur-Seine, France, 2007.

(2) (a) Stewart, D. A.; Rakich, J. V.; Lanfranco, M. J. NASA Report CP-2283, part 2; **1983**; p. 827; (b) Stewart, D. A.; Chen, Y. K.; Banford, B. J.; Romanowsky, A. B. *AIAA* **1995**, *95*, 2013. (c) Stewart, D. A.; Rakich, J. V.; Lanfranco, M. J. *AIAA* **1982**, *82*, 248.

(3) Scott, C. D. *AIAA* **1981**, *77*, 192.

(4) Balat-Pichelin, M.; Badie, J. M.; Berjoan, R.; Boubert, P. *Chem. Phys.* **2003**, *291*, 181.

(5) Watanabe, K.; Tatsumi, T. *Appl. Phys. Lett.* **2000**, *76*, 2940.

(6) Orellana, W.; da Silva, O. J. R.; Fazzio, A. *Phys. Rev. B* **2004**, *70*, 125206.

(7) Barker, J. A.; Auerbach, D. J. *Surf. Sci. Rep.* **1985**, *4*, 1.

(8) Schlichting, H.; Menzel, D.; Brunner, T.; Brenig, W. *J. Chem. Phys.* **1992**, *97*, 4453.

(9) Kim, Y. C.; Boudart, M. *Langmuir* **1991**, *7*, 2999.

(10) Guerra, V.; Loureiro, J. *Plasma Sources Sci. Technol.* **2004**, *13*, 85.

(11) Nasuti, F.; Barbato, M.; Bruno, C. *J. Thermophys. Heat Transfer* **1996**, *10*, 131.

(12) (a) Bedra, L.; Rutigliano, M.; Cacciatore, M.; Balat-Pichelin, M. *Langmuir* **2006**, *22*, 7208. (b) Cacciatore, M.; Rutigliano, M.; Billing, G. D. *J. Thermophys. Heat Transfer* **1999**, *13*, 195.

(13) Rutigliano, M.; Pieretti, A.; Cacciatore, M.; Sanna, N.; Barone, V. *Surf. Sci.* **2006**, *600*, 4239.

(14) Cacciatore, M.; Billing, G. D. *Surf. Sci.* **1990**, *232*, 35.

(15) Billing, G. D. *Dynamics of Molecule Surface Interactions*; Wiley: New York, 2000.

(16) See, for example: Dovesi, R.; Saunders, V. R.; Roetti, C.; Causà, M., Harrison, N. M.; Apra, E. *CRYSTAL 95 User's Manual*; University of Turin, Turin, Italy, 1996.

(17) Nakamura, K. G. *Chem. Phys. Lett.* **1998**, *285*, 21.

(18) Brivio, G. P.; Grimley, T. B. *Surf. Sci. Rep.* **1993**, *17*, 1.

(19) Dewar, M. J. S.; Thiel, W. *J. Am. Chem. Soc.* **1977**, *99*, 4899.

(20) Stewart, J. J. P. *J. Comput. Chem.* **1989**, *10*, 209.

(21) (a) Koch, W.; Holthousen, W. G. *A Chemist's Guide to Density Functional Theory*; Wiley-VCH, Weinheim, Germany, 2000. (b) Adamo, C.; Barone, V.; Di Matteo, A. *Adv. Quantum Chem.* **1999**, *36*, 45.

(22) Adamo, C.; Barone, V. *J. Chem. Phys.* **1999**, *110*, 6158.

(23) (a) Perdew, J. P.; Burke, K.; Ernzerhof, M. *Phys. Rev. Lett.* **1996**, *77*, 3865. (b) Perdew, J. P.; Burke, K.; Ernzerhof, M. *Phys. Rev. Lett.* **1997**, *78*, 1396.

(24) Herzberg G. In *Spectra of Diatomic Molecules, Molecular Spectra, and Molecular Structure*; Van Nostrand Reinhold: New York, 1950; Vol. 1.

(25) Krishnan, R.; Binkley, J. S.; Seeger, R.; Pople, J. A. *J. Chem. Phys.* **1980**, *72*, 650.

(26) Frisch, M. J.; Trucks, G. W.; Schlegel, H. B.; Scuseria, G. E.; Robb, M. A.; Cheeseman, J. R.; Montgomery, J. A., Jr.; Vreven, T.; Kudin, K. N.; Burant, J. C.; Millam, J. M.; Iyengar, S. S.; Tomasi, J.; Barone, V.; Mennucci, B.; Cossi, M.; Scalmani, G.; Rega, N.; Petersson, G. A.; Nakatsuji, H.; Hada, M.; Ehara, M.; Toyota, K.; Fukuda, R.; Hasegawa, J.; Ishida, M.; Nakajima, T.; Honda, Y.; Kitao, O.; Nakai, H.; Klene, M.; Li, X.; Knox, J. E.; Hratchian, H. P.; Cross, J. B.; Bakken, V.; Adamo, C.; Jaramillo, J.; Gomperts, R.; Stratmann, R. E.; Yazyev, O.; Austin, A. J.; Cammi, R.; Pomelli, C.; Ochterski, J. W.; Ayala, P. Y.; Morokuma, K.; Voth, G. A.; Salvador, P.; Dannenberg, J. J.; Zakrzewski, V. G.; Dapprich, S.; Daniels, A. D.; Strain, M. C.; Farkas, O.; Malick, D. K.; Rabuck, A. D.; Raghavachari, K.; Foresman, J. B.; Ortiz, J. V.; Cui, Q.; Baboul, A. G.; Clifford, S.; Cioslowski, J.; Stefanov, B. B.; Liu, G.; Liashenko, A.; Piskorz, P.; Komaromi, I.; Martin, R. L.; Fox, D. J.; Keith, T.; Al-Laham, M. A.; Peng, C. Y.; Nanayakkara, A.; Challacombe, M.; Gill, P. M. W.; Johnson, B.; Chen, W.; Wong, M. W.; Gonzalez, C.; Pople, J. A. *Gaussian 03*, revision C.02; Gaussian, Inc.: Wallingford, CT, 2004.

(27) (a) Rutigliano, M.; Cacciatore, M.; Billing, G. D. *Chem. Phys. Lett.* **2001**, *340*, 13. (b) Rutigliano, M.; Cacciatore, M. *ChemPhysChem* **2008**, *9*, 17.

(28) Cacciatore, M.; Christoffersen, E.; Rutigliano, M. *J. Phys. Chem. A* **2004**, *108*, 8810.

(29) Iannotta, S.; Gravili, C.; Boschetti, A.; Cagol, A.; Cacciatore, M. *Chem. Phys.* **1995**, *194*, 133.

(30) (a) Perdew, J. P.; Chevary, J. A.; Vosko, S. H.; Jackson, K. A.; Pederson, M. R.; Singh, D. J.; Fiolhais, C. *Phys. Rev. B* **1992**, *46*, 6671. (b) Perdew, J. P.; Wang, Y. *Phys. Rev. B* **1992**, *45*, 13244.

(31) (a) Arasa, C.; Busnego, H. F.; Salin, A.; Sayòs, R. *Surf. Sci.* **2008**, *602*, 975. (b) Arasa, C.; Gamallo, P.; Sayòs, R. *J. Phys. Chem. B* **2005**, *109*, 14954.

(32) Wyckoff, R. W. G. *Crystal Structures*; Interscience Publishers: New York, 1963.

(33) Feuston, B. P.; Garofalini, S. H. *J. Chem. Phys.* **1988**, *89*, 5818.

(34) Sen, P. N.; Thorpe, M F. *Phys. Rev. B* **1977**, *15*, 4030.

JP9066026